*Corresponding author's email:

aasifawa13@gmail.com

Indium-Tin Oxide (ITO) thin films deposited at low substrate temperature on bare corning glass substrates by RF sputtering: Structural and Electrical properties

Sanusi Abdullahi[1] and Abubakar A. Sifawa[2*]

To study the structural and electrical properties of Indium Tin Oxide (ITO) thin films, a set of ITO samples with different thicknesses were deposited by Radio Frequency (RF) sputtering technique. X-ray diffraction measurement shows that the crystal quality of ITO films was improved with the increase of film thickness and the annealing temperature. The resistivity decrease of ITO films with increase of film thickness owes to the change of carrier concentration for annealed thin films, and attributes to the improvement of the crystallinity.

Keywords: ITO, RF sputtering, sheet resistance, resistivity, bare corning glass

1.   Introduction

Indium tin oxide (ITO) is being widely used as transparent conductive electrode in applications such as flat panel displays and photovoltaic devices. Among the various deposition techniques, magnetron sputtering is the most widely used method due to its capability to coat on various substrates with good uniformity. To prepare ITO thin films that are suitable for use in different applications, major efforts have been made to improve the film properties such as conductivity, transparency, surface morphology and thermal stability. Previous investigations showed the influence of the deposition parameters such as film thickness and the annealing conditions on the performance of ITO films.

Among all the deposition parameters, ambient gases, chamber pressure, deposition temperature, RF power or discharge power are the most influential parameters: the ambient gases have a great impact on the chemical bonding states of the composing elements at the presence of either an oxidation ambient (oxygen) or a reduction ambient (hydrogen); the deposition pressure and temperature together determine the morphology, microstructure and crystallographic orientation of the thin films; while the deposition power influences the deposition rate and thus energy distribution of the species. Many methods have been employed to deposit ITO as a thin film. These methods include RF/DC sputtering [1-7], ion-beam sputter [8], e-beam evaporation [9-11], Spin coating [12] and sol-gel [13]. RF magnetron sputtering exhibits interesting advantages such as low substrate temperature, good adhesion of the films on the substrates, and a high deposition rate. In the present work, a report on the structural and the electrical properties of ITO films prepared by RF sputtering technique is presented.

2.   Methodology

2.1   Experimental Details

2.1.1   *The Sputtering mechanism*

The sputtering phenomenon known since 1852, has been exploited for deposition of films form non-conducting targets. During the sputtering process, an ion approaches the surface of a solid (target), the impact of which may set up a series of collisions between atoms of the target, leading to the ejection of one of these atoms. When an ion with energy of more than about 30 eV hits a surface, a small fraction of the energy and momentum of the incoming ion will, through lattice collisions, be reversed and may cause ejection of surface atoms.

The sputtered atoms leave the target surface with high energies ($\sim$10 eV) compared with evaporation atoms ($\sim$0.1 eV). The average number of the atoms ejected from the surface per incident ion is called the sputtering yield (S) which depends on many factors, such as the mass and the energy of the incident particles, the mass and the binding energy of the sputtered

atoms and the crystallinity of the target. The ion source is usually a plasma which is an electrically neutral mixture of positive ions and electrons generated by electron impact in a noble gas such as argon at sub-atmospheric pressures (typically 2 to 10 Pa). The ions are accelerated in an electric field obtained by applying a negative potential with respect to the plasma potential to an electrode immersed in that plasma. The ejected or sputtered atoms condenses on a substrate to form a thin film.

2.1.2   *Growth of the ITO thin films*

The ITO thin films were deposited on the bare corning glass substrate by RF-sputtering. The deposition was performed in a chamber of 12 inches in diameter using 4N pure ITO target (2 inches in diameter and 5 mm thickness). The substrates were cleaned using deionized water, acetone, and isopropyl alcohol under ultrasonic vibrations for 15 minutes. After drying substrates in hot air, the target and substrate were fixed in target holder and substrate holder, respectively, adjusting in such a way that the substrate surface was parallel to the target surface. The distance between the target and the substrate was maintained at 7cm. The sputter vacuum chamber was exiled to 2×10^5 mTorr. Argon gas flow rate was maintained at 20 sccm.

The operating pressure during sputtering was maintained at 9 mTorr, the RF power used was 75 W at radio frequency of 13.56 MHz. Pre-sputtering was carried out for 10 minutes to eliminate surface contamination of the target. The substrate temperature was kept constant at 100^0C while being rotated during the deposition at 35rpm. The 40 nm as-deposited, 40 nm annealed, 60 nm as-deposited and the 60 nm annealed are labelled as samples A, B, C and D respectively.

2.1.3   *Annealing of the samples*

After the deposition, the samples were annealed under nitrogen atmosphere at 1×10^{-4} Pa at 250^0C for 1 hour.

2.1.4   *Characterization of the samples*

The structural properties of thin films were analyzed by high-resolution X-ray diffraction (XRD – SIEMENS Diffractometer D5000) operated at 40 kV and 30 mA with $Cu = K\alpha (1.5404)\ \mathring{A}$ as the radiation source. Diffractograms recorded data in the angular range of 10 to 70^0 with a scan speed of 1^0/minute. The electrical properties of the

samples were examined by four-point probe (Keithley model 181 nanovolt electrometer). A probe head with tungsten carbide tips with a point radius of 0.002", a probe spacing of 0.05" and a probe pressure of 70 to 180 grams was used for all measurements. Current was supplied by a Crytronics model 120 current source with a range of applied currents between 1μA to 100 mA. Voltages were measured by a Keithley model 181 nanovolt electrometer with an input impedance of greater than 1 GΩ. All the characterizations were done at room temperature. The samples were labelled as A, B, C and D for 40nm as-deposited, 40nm annealed, 60nm as-deposited and 60nm annealed.

2.2   Data Analysis

The lattice parameters (a) and (c) of hexagonal phase and inter-planner spacing (d) were evaluated using Equations (1) and (2) by [14].

$$a = \frac{\lambda}{\sqrt{3}\ sin\ \theta} \tag{1}$$

and

$$c = \frac{k\lambda}{\beta Cos\ \theta} \tag{2}$$

Where a is the lattice parameter, λ wavelength of the incident radiation, β Full Width at Half Maximum (FWHM) of the preferential plane and θ Bragg's angle
The grain size (D) was estimated using Debye–Scherrer's formula by Equation (3) by [15].

$$D = \frac{\theta.9\lambda}{\beta\cos\theta} \tag{3}$$

Where D is the grain size, λ wavelength of the incident radiation, β Full Width at Half Maximum (FWHM) of the preferential plane and θ Bragg's angle. Dislocation density (σ) shows the dislocation or crystallographic defect within a crystal structure. It usually increases with plastic deformation and is determined [16] from equation (4),

$$\sigma = \frac{1}{D^2} \tag{4}$$

Where σ is the Dislocation Density and D is the grain size
The strain (ε) in thin films is defined as the disarrangement of lattice which is created during the deposition process and was calculated using Equation (5) from [17];

$$\varepsilon_{2(\%)} = \frac{c - c_0}{c_0} \times 100\% \tag{5}$$

With ε as the strain, c is the lattice parameter, C_0 is unstrained lattice parameter for bulk ITO. The resistivity and the sheet resistance of the ITO thin films were measured according to Equations (3) and (4) given by [6];

$$\rho = R_S \times t \qquad (6)$$

Where R_S is the sheet resistance and t is the film thickness.

3.   Results and Discussion

A typical XRD pattern of the as-deposited (samples A and C) and annealed (samples B and D) ITO film is shown in Figure 1. The standard pattern (PDF no. 06-0416) is used for comparison. The amorphous nature of the XRD scans is attributed to the amorphous glass substrate. The pattern shows two major diffraction peaks of (222) and (400) Miller planes. All the samples show a weak (222) texture which is attributed to low surface energy. Samples A and B show a (400) peak of high intensity. The absence of any sharp diffraction peaks in XRD patterns of samples C and D indicates the partially amorphous nature of these films.
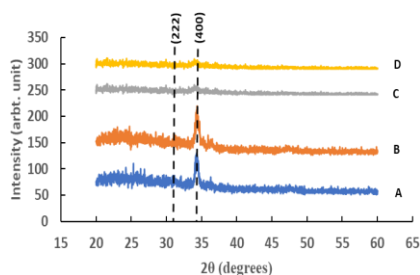

Figure 1. X-ray diffraction profile measured for RF-sputtered ITO thin films deposited on glass substrate at 100 °C.

Table 1 gives some of the structural constants such as FWHM, d-spacing, crystallite size, micro strain and dislocation density of the deposited ITO thin films. It can be observed from the table that the magnitude of the 2θ for the 40nm annealed sample decreased to 2θ=34.19º if compared with that of the as-deposited sample of the same thickness. The reason may be increase in particle size (reported somewhere else) as a result of the annealing. The d-spacing can be described as the distance between planes of atoms give rise to the diffraction peaks. The d-spacing of the 40nm as-deposited and annealed samples varies as a result of the annealing. For the 60nm thick samples, the d-spacing remain the same. From the crystallite sizes shown in table 1, there is a sharp decrease in the particle size of the 40nm annealed sample if compared with 40nm as-deposited sample. In the case of the 60nm as-deposited sample, an increase of the crystallite size has been observed which is always attributed to factors such as annealing. The observed improvement in crystallite size in the 60nm samples may also be attributed to strain formed in the nano crystal. The strain arises due to point defects (vacancies, site disorder), dislocations and extended defects in the crystal structures. Table 1 also shows that strain increases from 0.50 for the as-deposited sample to 0.70 for the annealed sample which is another manifestation of annealing. There is no change in both as-deposited and annealed samples of 60nm thickness. The dislocation density is to measure the disorder of lattice planes in the crystal structure. Information available in table 1 also shows that in all the samples analyzed, film thickness has also shown its influence on both the 40nm and the 60nm as-deposited and annealed samples.

Table 1. Structural constants of the deposited ITO thin films

Sample	2θ (degrees)	FWHM	d-spacing	Crystallite size (D)	Micro strain	Dislocation density
A	38.13	0.4093	2.36	234.29	0.50	1.82×10^{-5}
B	34.19	0.5038	2.62	187.46	0.70	2.84×10^{-5}
C	34.02	1.15	2.63	61.99	2.12	0.26×10^{-5}
D	34.02	1.15	2.63	71.99	2.12	0.19×10^{-5}

Electrical properties of ITO thin films depend on film combination and deposition parameters such as sputtering power, oxygen flow rate, substrate temperature, post deposition temperature etc. The resistivity of sample A is about 4.5×10^{-4} Ωcm while that of sample B is determined at 5.4×10^{-4} Ωcm. The resistivities of samples C and D are 3.6×10^{-4} Ωcm and 4.3 $\times$ 10^{-4} Ωcm respectively. The increase in resistivity as a result of annealing observed in samples B and D may be caused by the removal of oxygen vacancies by the chemisorbed oxygen and the formation of grain boundaries acting as trap sites for free electrons [18]. It can be seen that increase in thickness results in the decrease in resistivity. [4] suggested that decrease in the

ITO film resistance is attributed to crystallization. Again, crystallinity, high oxygen vacancy concentration, and grain growth, which reduces grain boundary scattering and surface roughness can result in reduced resistivity as suggested by [19]. The sheet resistance of sample A is 28 Ω/sq while that of sample B is 12 Ω/sq. The sheet resistance of samples C and D are 20 Ω/sq and 18 Ω/sq respectively. Electrical property of films was found to be related to the microstructure and crystallographic structure, which in turn strongly depend on the annealing temperature [20].

4.   Conclusion

In summary, ITO thin films were deposited by RF sputtering method on bare corning glass substrates. After the deposition, the films were then annealed in a furnace at 250^0C under N_2 atmosphere. The XRD results reveal that the annealed thin film has a good polycrystalline structure better than the as-deposited of 40 and 60 nm thickness. The electrical resistivity of the films increases after annealing. Finally, it can be said that the samples have potential applications in opto-electrical applications and in the field of photovoltaic cells.

Conflict of interest

The authors declare no conflict of interest.

References

[1]   Y. Wang, C. Zhang, J. Li, G. Ding and L. Duan, "Fabrication and characterization of ITO thin film resistance temperature detector" *Vacuum* xxx, 2016.

[2]   L. Voisin, M. Ohtsuka, S. Petrovska, R. Sergiienko and T. Nakamura, "Structural, optical and electrical properties of DC sputtered indium saving indium-tin oxide (ITO) thin films", *Optik - International Journal for Light and Electron Optics,* 2017.

[3]   A. Tamanai, Dao, T. D, Sendner, M, Nagao, T and A. Pucci, "Mid-infrared optical and electrical properties of indium tin oxide films", P*hys. Status Solidi A*, pp 1–8, 2016.

[4]   K. P Sibin, N. Swain, P. Chowdhury, A. Dev, N. Sridhara, H. D. Shashikala, A. KSharma, C. Harish and C. Barshilia, "Optical and electrical properties of ITO thin films sputtered on flexible FEP substrate as passive thermal control system for space applications" *Solar Energy Materials & Solar Cells* vol 145, pp 314–322, 2016.

[5]   J. Shin and W. Cho, (2018) "Microwave Annealing Effects of Indium-Tin-Oxide Thin Films: Comparison with Conventional Annealing Methods", *Phys. Status Solidi A,* pp 1-6, 2018.

[6]   M. Russak and J. Carlo (1983) "Radiofrequency sputtered indium tin oxide thin films" *Journal of Vacuum Science & Technology A* vol 1, pp 1563- 1584, 1983.

[7]   S. Isik, O. Coban, C. Shafai, S. Tuzemen and E. Gur "Growth conditions effects on the H_2 and CO_2 gas sensing properties of Indium Tin Oxide" *J. Phys.: Conf.* pp 1-8, 2016.

[8]   S. Venkatachalam, H. Nanjo, M. B. H. Fathy, K. Kazunori, W. Yoshito, H. Hiromichi and T. Ebina (2011). "Properties of Indium Tin Oxide Thin Films Deposited on Glass and Clay Substrates by Ion-Beam Sputter Deposition Method", *Japanese Journal of Applied Physics,* vol 50, pp 1-4, 2011.

[9]   R. X. Wang, C. D. Beling, S. Fung, A. B. Djurisˇicˊ, C. C. Ling, C. Kwong and S. Li "Influence of annealing temperature and environment on the properties of indium tin oxide thin films" *J. Phys. D: Appl. Phys.* Vol 38 (2005) 2000–2005, 2005.

[10]   J. K. Sheu, Y. K. Su, G. C. Chi, M. J. Jou and C. M. Chang "Effects of thermal annealing on the indium tin oxide Schottky contacts of n-GaN", *Applied Physics Letters* vol 72, 1998.

[11]   N. Mori, S. Ooki, N. Masubuchi, A. Tanaka, M. Kogoma and T. Ito "Effects of post-annealing in ozone environment on opto-electrical properties of Sn-doped In_2O_3 thin films" *Thin Solid Films,* vol 411 (2002) pp 6–11, 2002.

[12]   T. L. O. Sunde, E. Garskaite, B. Otter, H. E. Fossheim, R. Sæterli, R. Holmestad, M. Einarsrud, M and T. Grande "Transparent and conducting ITO thin films by spin coating of an aqueous precursor solution", *J. Mater. Chem,* vol 22, (2012), pp 15740, 2012.

[13]   M. Misra, D. Hwang, Y. C. Kim, J. Myoung and T. Lee, T. "Eco-friendly Method of Fabricating Indium-Tin- Oxide Thin Films using Pure Aqueous Sol-gel, *Ceramics International,* Vol 38 (2005), pp 2000–2005, 2017.

[14]   A. Purohit, S. Chander, S. Anshu, S. P. Nehra and M. S. Dhaka "Impact of low temperature annealing on structural, optical, electrical and morphological properties of ZnO thin films grown by RF sputtering for photovoltaic applications", *Optical Materials*, vol 49 (2015), pp 51–58, 2015.

[15] S. Abdullahi, M. Momoh and K. U. Isah "Electrical and Structural Properties of Radio Frequency (RF) Sputtered ZnO Thin Film at Low Substrate Temperature", *Journal of Electrical Engineering* vol 2 (2014), pp 12-19, 2014.

[16] I. Illican, Y. Caglar and M. Caglar "Structure, Morphological and optical properties of $CuAlS_2$ films prepared by Spray Pyrolysis", *Journal of Optoelectronics and advanced Materials*, vol 10 (10), 2008.

[17] S. Abdullahi, M. Momoh, A. U. Moreh, G. M. Argungu, A. Bala, S. Namadi, M. B. Abdullahi and B. A. Maiyama "The Role of Air Annealing on the Structural and Electrical Properties of Zinc Oxide (ZnO) Thin Film Deposited by Rf Sputtering Technique", *Sch. J. Eng. Tech,* vol 5 (12), pp 704-708, Dec 2017.

[18] H. A. Mohamed and H. M. Ali "Characterization of ITO/CdO/glass thin films evaporated by electron beam technique", *Sci. Technol. Adv. Mater.* Vol 9 (2008), pp 9, 2008.

[19] M. K. M Ali, K. Ibrahim, O. S. Hamad, M. H. Eisa, M. G. Faraj and F. Azhari "Deposited Indium Tin Oxide (ITO) thin films by DC-magnetron sputtering on Polyethylene Terephthalate substrate (PTE)", *Rom. Journ. Phys*, vol 56, (5–6), pp 730–741, 2011.

[20] M. H. Habibi and N. Talebian "The Effect of Annealing on Structural, Optical and Electrical Properties of Nanostructured Tin Doped Indium Oxide Thin Films", *Acta Chim. Slov.* vol 53 (2005), pp 53–59, 2005.